Arab J Geosci (2015) 8:7191–7206
DOI 10.1007/s12517-014-1701-7

ORIGINAL PAPER

Mafic enclaves in north of Urumieh plutonic complex: evidence of magma mixing and mingling, Sanandaj–Sirjan zone, NW Iran

Amin Jafari · Abdolnaser Fazlnia · Susan Jamei

Received: 29 April 2014 / Accepted: 4 November 2014 / Published online: 14 November 2014

Abstract The felsic granitoids in the north of Urumieh plutonic complex are associated with abundant mafic rocks as mafic microgranular enclaves (MMEs). Typically, mafic enclaves are gabbrodiorite and monzo-gabbro/diorite in composition, and they are hosted by quartz syenite. MMEs have variable size (from a few centimeters up to 4 m) and shapes (including rounded, ellipsoidal, discoidal, lenticular, tabular, and elongated). MMEs, structurally and petrographically are characterized by irregular, gradual, and sharp contact surfaces, finer-grained enclaves and areas enriched in mafic material, feldspar phenocrysts in enclaves, plagioclase zoning with resorbed rims, acicular apatite, blade-like biotite, and mafic clots, indicating mixing and mingling of co-existing mafic and felsic magmas with liquid–liquid relation. MMEs generally contain higher values of Fe_2O_3, MgO, CaO, TiO_2, MnO, V, Co, U, Sr, Nb, Ta, Ti, P, and heavy earth elements (HREE) and lower values of Al_2O_3, Na_2O_3, K_2O, Ba, Rb, Th, K, Hf, and Zr than their host, which are in consistent with occurrence of abundant ferromagnesian minerals in the enclaves. Geochemically, the mafic enclaves and host are metaluminous with medium- to high-K calc-alkaline nature and strongly enriched in long ionic lithophile elements (LILE) and light earth elements (LREE) compared with high field strength elements (HFSE) and HREE. Some major and trace elements form linear trends on harker diagrams, having approximately identical concentration of trace elements, similar mineralogical composition, and high Mg no. in the both enclaves and host, suggesting their co-genetic origin. Our investigation shows that the enclave-forming magma may have originated from the uppermost metasomatized asthenospheric mantle and formed from a basaltic parent magma. Consequently, felsic part might have been produced by fractional crystallization from enclave-forming mafic magma in lithospheric mantle, supported by large volume of the mafic mass relative to the felsic unit. Finally, coeval mafic and felsic magmas may have mingled and mixed at two distinct, but continuous periods at different levels (before and during ascent and emplacement) as a result of combined multistage interactions (least and slight hybridization stages), which are commonly represented by basic to intermediate or hybrid MMEs.

Keywords Mafic microgranular enclaves · Magma mixing/mingling · Hybridization · Geochemistry · Petrogenesis

A. Jafari (✉) · A. Fazlnia · S. Jamei
Geology Department, Faulty of Science, Urmia University, Urmia, Islamic Republic of Iran
e-mail: amin.jafari2009@yahoo.com

A. Jafari
e-mail: a.jafari9291@gmail.com

Introduction

Mafic microgranular enclaves (MMEs) are common in intermediate and felsic plutons worldwide, particularly in calc-alkaline granitoids and play a substantial role in the evolution of granitic magmas. Characterization, genesis, and evolution of MMEs have been extensively discussed by several authors (e.g., Pabst 1928; Didier 1973; Hibbard 1981; Topley et al. 1982; Vernon 1983; Bacon 1986; Barbarin and Didier 1992). There are three main controversial models in petrogenesis of MMEs: (1) they formed by settling of early crystals from the host magma or fragments of early solidified wall-rock facies closely related to the host magma (cognate model) (e.g., Chappell et al. 1987; Dahlquist 2002; Ilbeyli and Pearce 2005), (2) they are recrystallized fragments, refractory metamorphic rocks, and residual fragments from a granitic source (restite model) (e.g., Chappel and White 1992; White et al. 1999), or (3) in generally they are hybridized magmas and globules of more mafic magma mixed with felsic host magma (hybridization model) (e.g., Vernon 1984; Barbarin 2005;

Feeley et al. 2008; Kaygusuz and Aydıncakır 2009). Among the three mentioned models, there are various discussions between researchers. Advocates of magma mixing attribute the compositional similarities between enclaves and host rocks to varying degrees of chemical equilibration and diffusional exchange between the co-existing magmas during slow cooling (Pin et al. 1990; Allen 1991; Holden et al. 1991). Didier and Barbarin (1991) and Vernon (1983, 1991) have challenged the "Restite Model" by making distinctions between restites and microgranular enclaves based on textural, mineralogical and chemical observations. Based on "cognate model," three different mechanisms have been proposed which are similar to geochemistry and isotopic characteristics of the microgranular enclaves and their host rocks are easily interpretable in terms of this hypothesis. These three mechanisms are (1) cumulate clots (Dodge and Kistler 1990; Dahlquist 2002), (2) disrupted chilled margins (Donaire et al. 2005), and (3) disrupted cumulate assemblages (Bebien 1991; Platevoet and Bonin 1991). Among the described models, the hybridism model, in particular has been well documented by many geologists (e.g., Frost and Mahood 1987; Didier and Barbarin 1991; Blundy and Sparks 1992; Silva et al. 2000; Barbarin 2005). Although the problems associated with magma mixing is still highly debated, this model, however, has been applied in studies of granites worldwide.

The aim of the present study is to investigate hybridization process between MMEs and host rock based on field and petrographic evidences, considering that studied host and its MMEs can be considered as an ideal opportunity to pursue these types of geological phenomena. In addition, the geochemical data were used to study chemical interaction between MMEs–host rocks and also specific magmatic processes which may have been involved in the genesis of the microgranular enclaves.

Geological background

The subduction of the Neo-Tethyan ocean floor beneath Iran sutured Iran to Arabia (e.g., Takin 1972; Berberian and King 1981; Alavi 1994), and the subsequent continental convergence built the Zagros orogenic belt. This orogenic belt is considered part of the Alpine orogenic system and consists of three NW-SE trending parallel zones: (1) Zagros fold–thrust belt (ZFTB), (2) Urumieh–Dokhtar magmatic assemblage (UDMA), and (3) Sanandaj–Sirjan zone (SSZ) (Alavi 1994) (Fig. 1).

The study area is located in the northwestern part of the SSZ. This zone is 150–200 km wide and 1500 km long and lies between the towns of Sirjan and Esfandagheh in the southeast and Urumieh and Sanandaj in the northwest (Mohajjel and Fergusson 2000) (Fig. 1). The SSZ is a central part of Zagros orogen (Alavi 1994) and forms part of the Tethys orogenic belt (Sengor 1990). During the Mesozoic, the Neotethys oceanic crust was subducted beneath the Eurasian Plate (Golonka 2004; Molinaro et al. 2005; Agard et al. 2011; Mouthereau et al. 2012) and the SSZ occupied the position of a magmatic arc (Agard et al. 2011; Mouthereau et al. 2012). The SSZ is characterized by metamorphic and complexly deformed rocks associated with abundant deformed and undeformed plutons in addition to widespread Mesozoic volcanic rocks (e.g., Azizi and Jahangiri 2008; Mohajjel et al. 2003). Palaeozoic rocks rarely exposed except in the southeast where they are common (Berberian 1977). Numerous granitoid intrusions have occurred in the SSZ which are mainly calc-alkaline and are most likely generated at an active margin or later over a subduction zone (Ricou 1994; Mohajjel and Fergusson 2000; Azizi and Jahangiri 2008). The granitoids are dominated by biotite-granite, biotite-hornblende granodiorite, and hornblende-biotite quartz-diorite. Mafic rocks are common, particularly to the north of the SSZ, and occur as separate bodies, or more commonly, associated with granitoids in composite bodies (Alirezaei and Hassanzadeh 2012). Most of the intrusions have been indicated at Jurassic–Paleocene times (e.g., Masoudi et al. 2002; Mohajjel et al. 2003; Nezafati et al. 2005; Shahbazi et al. 2010). Older magmatic activity in the SSZ includes Late Triassie and Early Jurassic tholeiitic mafic volcanic rocks (Alavi and Mahdavi 1994), which are interpreted as remnants of Tethyan oceanic crust and Late Proterozoic to Early Paleozoic mafic rocks which formed during earlier extindional events (Berberian and King 1981; Rachidnejad-Omran et al. 2002).

Field relation and structural evidence of magma mixing

The South-Urumieh plutonic complex is dominated by intrusive bodies and Paleozoic and Mesozoic sedimentary rocks. The complex consist of a wide variety of plutonic rock types, including gabbrodiorite, diorite, q-syenite, granite, along with intermediate rocks formed by magma mixing (Fig. 2). The dominant lithology of the complex has a mafic composition which locally cross-cut by dykes of granite and quartz syenite in different places and do not contain enclaves or xenoliths. The rocks with felsic affinities are relatively small igneous intrusions compared with mafic units and commonly contain mafic microgranular enclaves. All cited units intrude Permian to Jurassic sedimentary rocks, mainly limestones and shales and are overlain by Early Miocene formations (Fig. 2). Numerous faults of probable Cenozoic age cut the plutonic rocks and an overall rocks are tectonized as a result of different tectonic processes (Fig. 2). Structurally, dominant trends of faults, folds, and mountains are NW-SE which follow by SSZ direction. The presence of colored melange consisting of

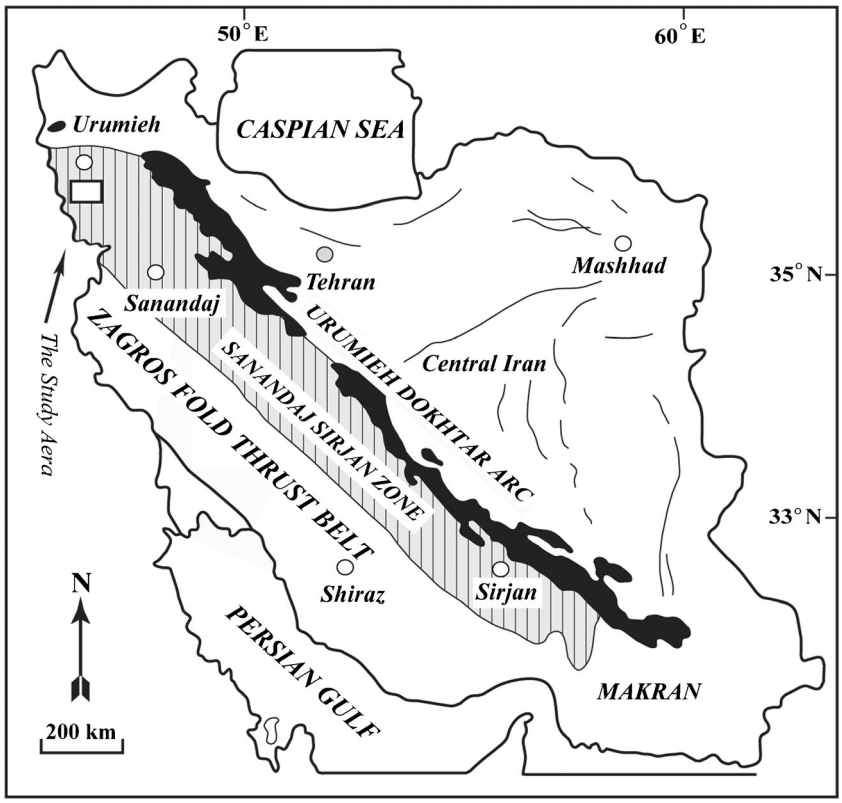

Fig. 1 The general tectonic map of Iran with separation of tree parallel zone: the Sanandaj–Sirjan zone (SSZ), the Urumieh-Dokhtar magmatic assemblage (UDMA), and the Zagros fold–thrust belt (ZFTB) (after Stocklin 1968; Alavi et al. 1997)

serpentinized pyroxenite, basic volcanic rocks, radiolarite, and pelagic limestone of Late Cretaceous to Eocene age, represent the remnants of the Neotethys oceanic lithosphere in the study area (Shahrabi and Saidi 1985; Naghizadeh and Ghalamghash 2005). Extensive magma mingling and mixing in most composite plutons in this region are clearly observed which imply to magmas interactions especially in the north area between Ghamishlu gabbrodiorite and Bardkish q-syenite (Fig. 2). Different types of MME can be distinguished between the last two cited units by their grain size, structure, mineral content, nature, composition, external morphology, and contacts with host granitoids. Mafic enclaves are distributed throughout the felsic pluton. Enclaves are gray to black colored and medium to fine grained while the host is light colored and medium to coarse grained. MMEs have variable size (ranges from a few centimeters up to 4 m) and shapes (including rounded, ellipsoidal, discoidal, lenticular, tabular, and with diverse elongated form) (Fig. 3a, b). Mafic enclaves are highly elongated due to stretching within the convecting felsic magma (Fig. 3a, b). Enclaves contact surface are sharp, straight, and crenulated. But in most cases, contact surface of MMEs with host granitoids are characterized with irregular and angled margins. In some cases, contact of mafic enclaves with host rocks is enriched in mafic material such as biotite and hornblende (Fig. 3c). Some mafic enclaves have a light-colored transitional zone at the contact with host rock (Fig. 3d). This is probably due to hybridization between the enclave-forming and host magmas. In most cases, MMEs margins are irregular and angled (Fig. 3e). Margins of some MMEs irrespective of morphology and size are more fine-grained and slightly darker (a few millimeters) near the contact with host granitoid which were created as a result of rapid cooling (Fig. 3e). In some MMEs, feldspar phenocrysts belong to host granitoid with variable amounts, shapes, and sizes and are shown to display partial dissolution (corroded) and overgrowth textures under relatively higher temperature of mafic–felsic (hybrid) magma (Fig. 3f).

Petrographic descriptions of mafic enclaves and host

Classification of the investigated host and its enclaves are shown on the QAP diagram of Streckeisen (1973) based on the modal abundance of minerals (Fig. 4). According to this nomenclature, MMEs range from gabbrodiorite to monzogabbro/diorite and are composed of plagioclase (45–50 %) and mafic minerals (40–50 %). MMEs approximately have a similar mineralogy with hypidiomorphic granular texture. They are composed predominantly of plagioclase, biotite, amphibole and clinopyroxene (four principal constituent), K-feldspar, and quartz. Titanite, apatite, zircon, and magnetite occur as accessory minerals, and some sericite, epidote, and chlorite are present as secondary phases in enclaves. In the MME, plagioclase in different sizes, as euhedral to subhedral

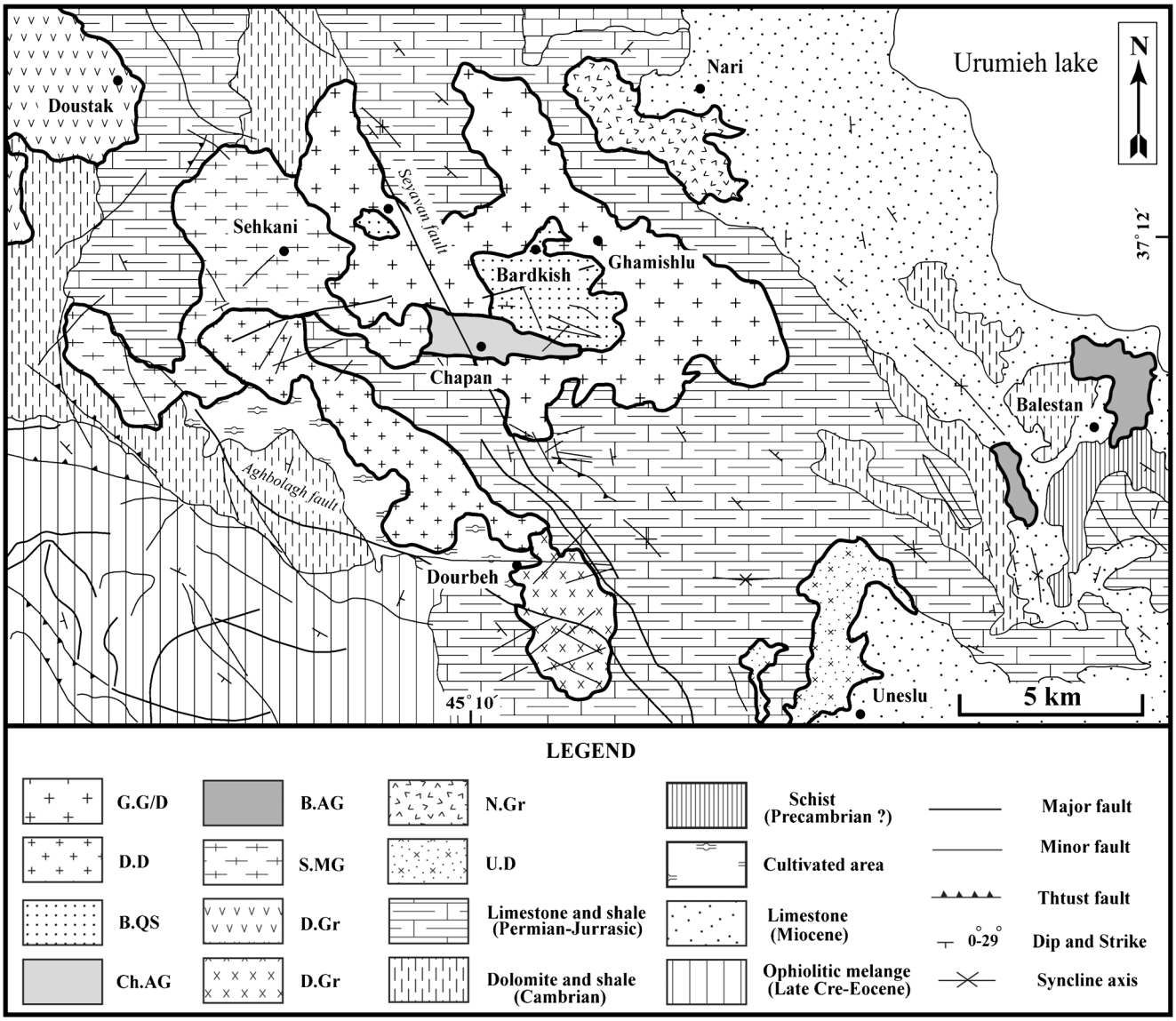

Fig. 2 Simplified geological map of south Urumieh plutonic complex. *G.G/D* Ghamishlu gabbrodiorite, *D.D* Dourbeh diorite, *D.U* Uneslu diorite, *B.QS* Bardkish q-syenite, *N.G* Nari granite, *S.G* Sehkani granite, *D.G* Dourbeh granite, *DG* Doustak granite, *Ch.AG* Chapan alkali-granite, *B.AG* Balestan alkali-granite

crystals are similar to those in the host granitoid and display nonequilibrium textures such as dissolved margins (Fig. 5a) and chemical zoning (Fig. 5b). Plagioclase commonly shows evidence of sericitization. Biotite occurs as anhedral to euhedral crystals and has a tabular to bladed appearance and is commonly altered to chlorite and opaque minerals (Fig. 5c). Amphibole is present as subhedral prisms and is often partly altered to chlorite and biotite. Subhedral K-feldspar (orthoclase) in different sizes occurs as phenocrysts, perthitic crystals and intergrowth with quartz. Fine accessory apatite as prismatic and acicular crystals occurs as inclusions in feldspars (Fig. 5d).

The host mass is classified modally as q-syenite (Fig. 4) and contains less plagioclase (20–25 %) and mafic minerals (5–10 %) and much more quartz and K-feldspar (55–65 %). The rocks have a porphyritic hypidiomorphic granular texture and consist primarily of K-feldspar and plagioclase as principal constituent minerals and quartz, biotite, and amphibole. Accessory amounts of fine-grained acicular apatite, titanite, magnetite anhedral oxide minerals, and chlorite and sericite are also locally present as secondary phases resulting from metasomatic processes. K-feldspar in different sizes occurs as anhedral to subhedral crystals. Potassium feldspars mainly are orthoclase and display Carlsbad twinning, perthite texture, and dissolved margins. Larger crystals of K-feldspar are embedded in finer-grained groundmass exhibiting porphyritic texture (Fig. 6a). Plagioclase in different sizes occurs in the form of euhedral to subhedral crystals, is characterized by zoning (Fig. 6b) and dissolved margins (Fig. 6c), and is affected by sericitization. Biotite is generally anhedral to

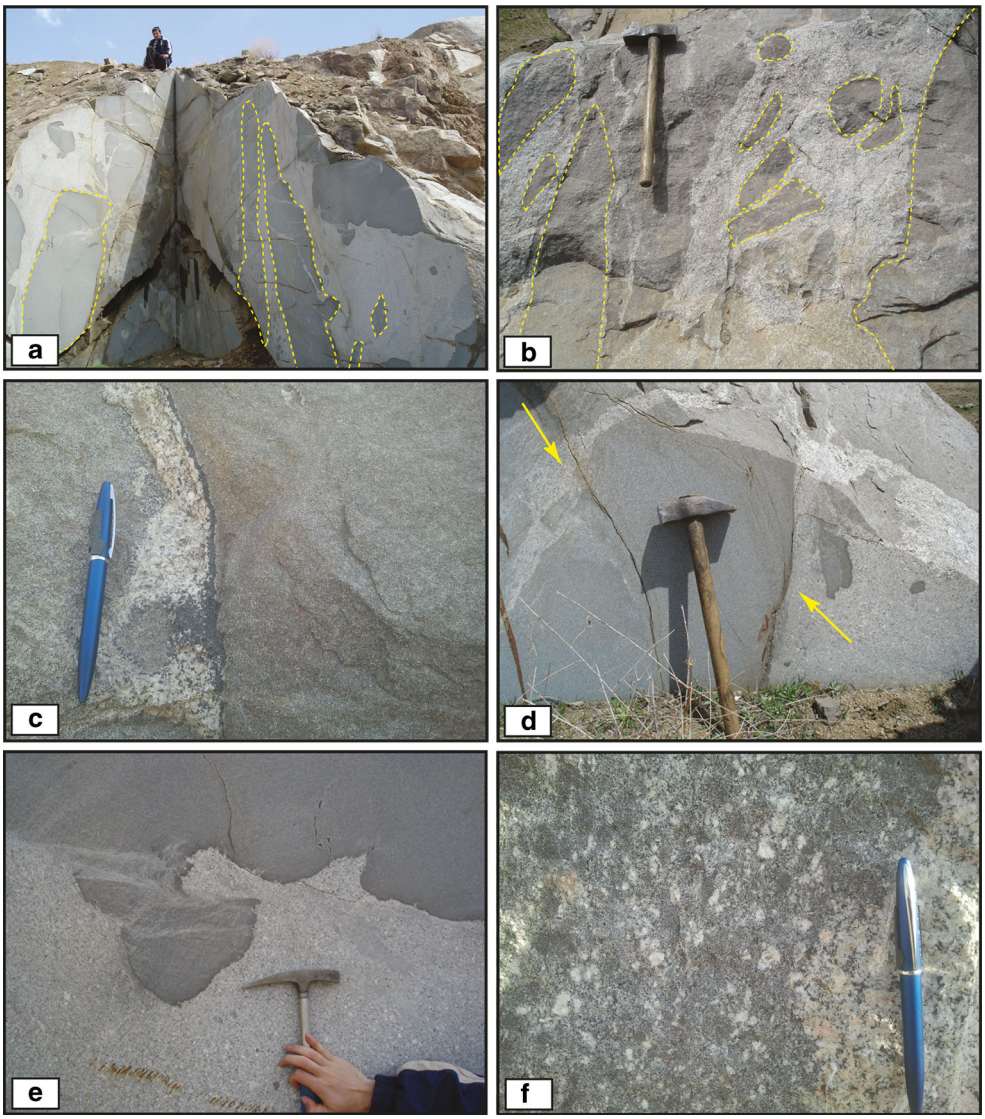

Fig. 3 **a**, **b** Mafic enclaves (ME) in different sizes and shapes into host; **c** ME showing a darker rim near enclave-host granitoid contact due to the growth of mafic minerals; **d** ME with both sharp and transitional zone at the contact with host rock; **e** fine-grained ME showing irregular margin; **f** feldspar phenocrysts owned to felsic host magma in ME

subhedral and often altered to titanite, chlorite, and iron oxides (Fig. 6d). Amphibole is present as subhedral prisms and in some places shows conversion to brown biotite and chlorite (Fig. 6d). Apatite as inclusions in feldspars has typical acicular shape, but stubby prismatic shapes also exist. Quartzes are fine to coarse grained and occur in interspaces between K-feldspar and plagioclase.

Analytical methods

The selected samples were analyzed for whole-rock major, trace, and rare earth elements compositions by ICP-emission spectrometry and ICP-mass spectrometry using natural rock standards as reference samples for calibration at ACME Analytical Laboratories in Vancouver, British Columbia, Canada. Table 1 presents whole rock major and trace element data for representative samples of enclaves and their host rocks.

Geochemistry

The SiO_2 content of the representative samples vary from 42 to 56 wt.% for enclaves (mafic to intermediate in composition) and 60 to 62 wt.% for host rocks (intermediate in composition) (Table 1). Given the AFM diagram (Irvine and Baragar 1971) (Fig. 7a), predominantly all samples lie in the calc-alkaline fields. According to A/CNK vs. A/NK diagram (Maniar and Piccoli 1989) (Fig. 7b), enclaves and host display I-type granitoid affinity with metaluminous nature (A/CNK <1.1, ranges from 0.65 to 0.98) (Table 1). The geochemical differences between mafic enclaves and felsic host rocks are shown in SiO_2 variation diagrams (Figs. 8 and 9). As seen in harker

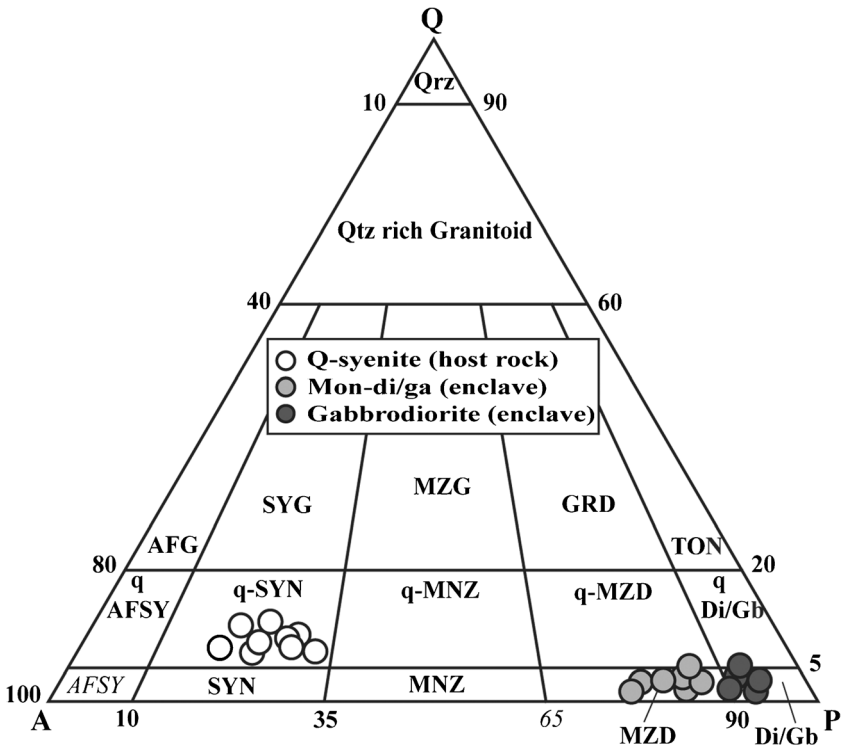

Fig. 4 Q-A-P ternary diagram (Streckeisen 1973)

diagrams, linear trends are apparent for the major and trace elements of the enclaves and host granitoid. Compared with the host, the mafic enclaves have higher Fe_2O_3, MgO, CaO, TiO_2, MnO, Sr, V, Co, and U contents. In addition, amount of Al_2O_3, Na_2O_3, K_2O, Rb, Zr, Th, and Ba in the host rocks are higher than enclaves (Figs. 8 and 9). These variations relative to SiO_2 are compatible with mineralogical observations.

Trace element distribution patterns for the enclaves and hosts are normalized to chondrites following Thompson (1982) (Fig. 10a, b). According to REEs diagram (Fig. 10a), both enclaves and their host display negative slope from light earth elements (LREE) to heavy earth elements (HREE) (La_N/Yb_N ratios ranging from 11.83 to 37.06) except for Ho which indicates highlight positive anomaly, relatively flat and undifferentiated patterns of HREE (Gd_n/Yb_n 1.67–2.32). The REE patterns of the enclaves are similar to host granitoids, but microgranular enclaves generally have higher contents of all REE (except for some LREE such as La, Ce, and Pr), higher Gd_n/Yb_n and Sm_n/Yb_n (Table 1). Furthermore, MMEs display some negligible to slightly negative Eu anomalies (Eu/Eu*= 0.75–1.04) and are approximately similar to the host granitoid (Eu/Eu*=0.95–1.45).

Considering multielement spider diagram (Fig. 10b), as a first approximation, MMEs and hosts are generally enriched in the most long ionic lithophile elements (LILE; e.g., Rb, Ba, Th, La, and Ce) and LREE relative to high field strength elements or (HFSE; e.g., Nb, Ti, Zr, and P) and HREE. However, despite the overall similarity, they exhibit a slight difference in trace element concentrations. MMEs indicate an obvious depletion in some LILEs, such as Ba, Rb, Th, and K relative to the host. In addition, some HFSE such as Hf and Zr depleted and some HFSE such as Nb, Ta, Ti, and P enriched in the mafic enclaves in comparison with their host. Although trace elements abundance of the MMEs and their host rocks are slightly different and there are some differences in the peaks and troughs, both of them display similar characteristics, indicating a single magmatic process in generation of the rocks. The trace element concentration (high LREE and LILE than HREE and HFSE) in all sample rocks are compatible with typical of arc magmatism (e.g., Parada et al. 1999; Shaw et al. 1993). An active continental margin setting conforms to the calc-alkaline character of the samples, with lower crust possible origin. In summary, the behavior of some major and trace elements with continuous trends on harker diagrams plus similar patterns on spider diagrams confirm that chemical variations among enclaves are explained by magmatic differentiation mechanisms.

The behavior of major, trace, and REE reflects element exchange between the MMEs and felsic host rocks. This diffusional element mobility is thought to be due to thermal, mechanical, and chemical (compositional) interactions between the coeval felsic and mafic magmas. Thermal exchange is much more rapid than mechanical or chemical exchange (Barbarin and Didier 1992). Chemical exchange generally acts after thermal equilibration, because the rate of thermal diffusion is typically three to five orders of magnitude larger than chemical diffusion in silicate melts (Fernandez and Barbarin 1991; Barbarin and Didier 1992). Especially, the

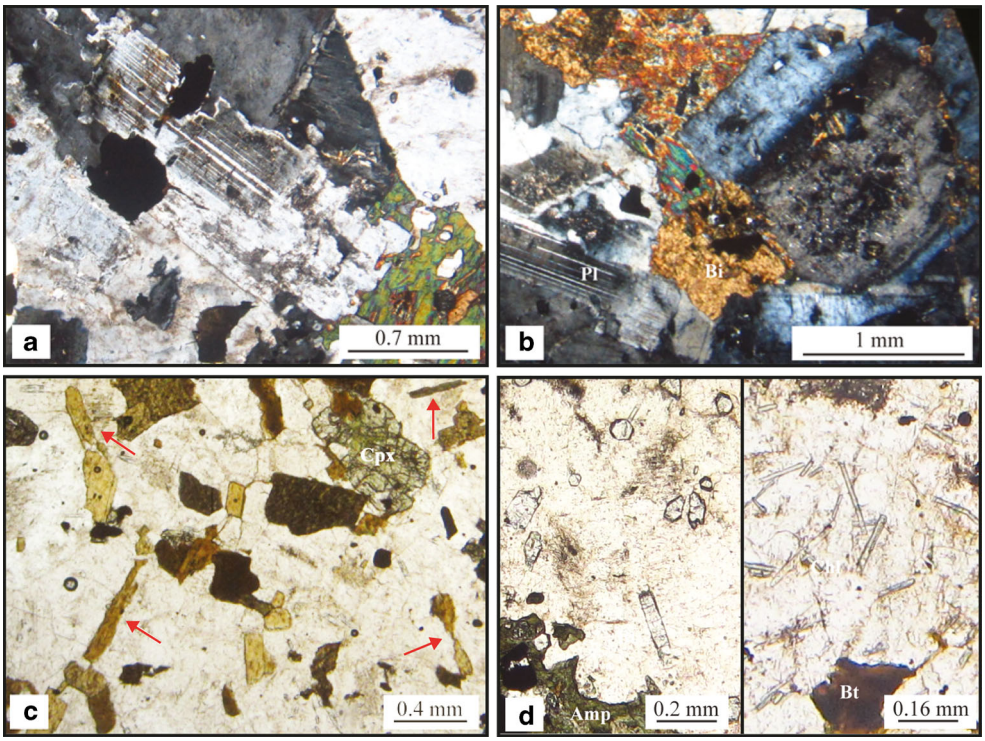

Fig. 5 **a** A plagioclase showing dissolved margins; **b** sector zoning of a plagioclase; **c** tabular to bladed appearance of biotites; **d** acicular and prismatic crystals of apatite as inclusions in feldspars

mutual exchange of major elements by diffusion leads to a differential migration of all elements on both sides of the contact surface. This selective two-way diffusion is significantly enhanced by the presence of fluid phases, especially of H_2O (Barbarin and Didier 1992). The mafic enclaves in the study area are characterized by the great abundance of hydrous minerals (such as hornblende and biotite). This, together with concentration of mafic minerals in mafic and felsic magma contact surfaces (Fig. 3c) strongly suggests that the migration of fluids from the host felsic magma to enclaves was effective. During the processes of fluid influx, chemical transfer of some mobile elements would be inevitable. The

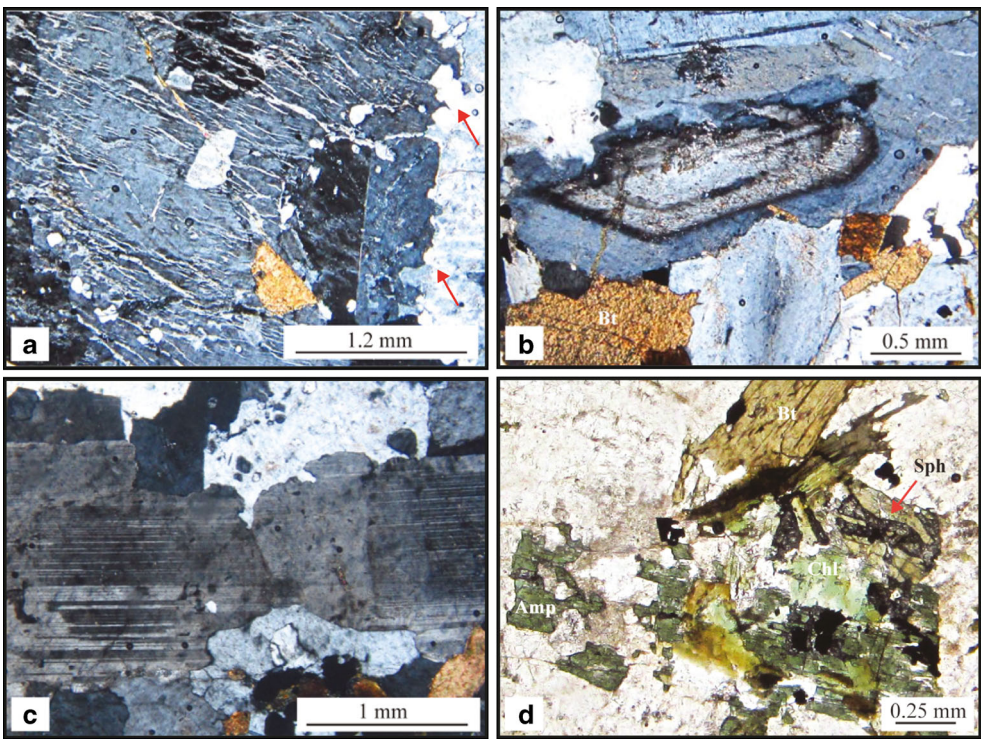

Fig. 6 **a** Perthitic orthoclase phenocryst indicating resorbed rim and contains inclusions of quartz and biotite; **b** a plagioclase crystal with chemical zoning; **c** marginal dissolution of a plagioclase crystal; **d** mafic clots of intergrown biotite, amphibole, showing alteration to secondary biotite, chlorite, titanite, and iron oxides

Table 1 Whole rock major (wt.%) and trace (ppm) element results of enclaves and their host rocks

Composition	Early mafic enclaves Gabbrodiorite		Hybrid enclaves Monzo-gabbro/diorite			Host rocks Q-syenite			
Sample	Cj-42	Cj-44	Cj-40	Cj-41	Cj-43	Cj-45	Cj-46	Cj-47	Cj-48
SiO_2	47.27	42.68	54.68	56.34	55.51	62.07	62.43	61.25	60.99
TiO_2	3.19	3.78	1.94	1.64	1.73	0.75	0.62	0.75	0.66
Al_2O_2	16.37	15.94	16.9	17.38	17.74	18.01	17.95	17.82	18.73
Cr_2O_3	0.015	0.014	0.02	0.021	0.023	0.03	0.033	0.035	0.03
tFe_2O_3	14.3	16.94	8.17	7.6	7.94	4.7	4.24	5.13	4.43
FeO*	12.86	15.24	7.35	6.83	7.14	4.22	3.81	4.61	3.98
MnO	0.19	0.2	0.16	0.17	0.18	0.11	0.08	0.09	0.09
MgO	3.82	4.33	2.87	2.48	2.54	1.04	0.88	1.13	0.92
CaO	6.53	8.89	5.77	5.24	5.49	2.79	2.43	2.8	2.9
Na_2O	3.97	3.56	4.6	5.23	5.65	5.17	4.53	4.8	5.4
K_2O	2.42	1.98	2.92	2.21	1.7	4.56	5.94	5.21	4.58
P_2O_2	0.67	0.56	0.6	0.66	0.69	0.21	0.18	0.2	0.18
LOI	0.9	0.8	1.1	0.8	0.6	0.3	0.4	0.5	0.8
Total	99.645	99.674	99.73	99.771	99.793	99.74	99.713	99.715	99.71
Ba	474	422	575	408	235	1083	1328	1163	1158
Rb	71.1	52.8	111.0	74.4	59.0	109.7	126.5	130.7	89.3
Sr	510.4	562.0	451.3	426.6	415.3	354.0	367.8	390.4	367.8
Y	23.6	21.9	24.2	28.6	29.1	18.8	10.6	17.3	13.5
Zr	186.1	172.5	253.4	73.9	274.3	377.6	362.8	476.0	441.1
Nb	59.3	48.5	62.4	90.4	74.5	52.3	28.0	43.2	36.4
Th	14.1	14.1	14.1	14.1	14.1	14.1	14.1	14.1	14.1
Pb	1.0	0.9	1.3	1.0	1.1	1.8	1.9	1.9	1.7
Ga	21.7	22.2	19.4	19.3	19.7	20.5	17.6	22.7	21.4
Zn	81	100	64	51	55	51	31	39	40
Cu	22.4	40.8	10.7	10.0	11.6	3.2	2.3	3.6	2.4
Ni	11.0	19.9	3.5	1.7	1.5	2.6	2.4	2.3	2.8
V	414	552	166	112	116	41	40	60	39
Cr	102.64	95.80	136.86	143.70	157.38	205.29	225.81	239.505	205.29
Hf	4.7	3.9	5.9	2.2	6.4	8.1	8.3	10.2	9.4
Cs	0.8	1.5	1.0	1.2	0.9	1.2	0.9	0.9	0.7
Ta	3.7	2.8	4.1	4.4	3.9	2.7	1.5	2.4	2.0
Co	32.4	44.2	15.9	11.6	11.6	5.0	5.2	6.2	4.6
U	1.5	1.1	2.3	1.4	1.7	1.9	1.8	2.3	2.2
Sn	2	1	1	2	2	1	<1	2	1
La	39.8	35.1	46.3	58.7	55.4	88.5	60.2	88.4	87.4
Ce	75.4	65.9	83.4	105.8	99.2	135.5	87.7	134.9	130.6
Pr	8.54	7.65	9.30	11.88	10.97	12.10	7.82	11.70	11.26
Nd	33.7	27.5	33.3	43.7	40.9	37.6	23.6	34.7	33.9
Sm	5.96	5.64	6.05	7.82	7.23	4.96	2.88	4.92	4.07
Eu	1.96	1.74	1.78	1.83	1.79	1.40	1.27	1.52	1.52
Gd	5.59	4.94	5.42	7.03	6.42	4.12	2.49	3.77	3.30
Tb	0.76	0.72	0.80	1.01	0.89	0.56	0.33	0.51	0.43
Dy	4.17	4.06	4.26	5.68	5.23	3.42	1.90	3.28	2.44
Ho	0.92	0.78	0.91	1.11	1.05	0.64	0.37	0.64	0.44
Er	2.18	2.12	2.44	2.73	2.64	1.82	1.06	1.72	1.37
Tm	0.34	0.31	0.34	0.40	0.41	0.30	0.16	0.27	0.22

Table 1 (continued)

Composition	Early mafic enclaves Gabbrodiorite		Hybrid enclaves Monzo-gabbro/diorite			Host rocks Q-syenite			
Sample	Cj-42	Cj-44	Cj-40	Cj-41	Cj-43	Cj-45	Cj-46	Cj-47	Cj-48
Yb	2.08	2.00	2.44	2.44	2.43	1.80	1.19	1.64	1.59
Lu	0.30	0.28	0.35	0.37	0.40	0.31	0.21	0.31	0.28
K	20090.84	16437.96	24241.84	18347.42	14113.40	37857.12	49313.88	43253.42	38023.16
Ti	19124.05	22661.10	11630.30	9831.80	10371.35	4496.25	3716.90	4496.25	3956.70
P	2924.01	2443.95	2618.52	2880.37	3011.30	916.48	785.56	872.84	785.56
Mg no.	36.6	33.61	41.03	39.26	38.79	30.47	29.13	30.38	29.14
A/CNK	0.77	0.65	0.79	0.84	0.84	0.97	0.98	0.95	0.97
Eu/Eu*	1.04	1.01	0.95	0.75	0.8	0.95	1.45	1.08	1.27
La_n/Yb_n	12.9	11.83	12.79	16.22	15.37	33.14	34.11	36.34	37.06
La_n/Sm_n	4.2	3.91	4.81	4.72	4.82	11.22	13.15	11.3	13.51
Gd_n/Yb_n	2.16	1.99	1.79	2.32	2.13	1.84	1.68	1.85	1.67
Sm_n/Yb_n	3.07	3.02	2.65	3.43	3.18	2.95	2.59	3.21	2.74

$Eu/Eu^* = (Eu/Eu_N)/[\sqrt{(Sm/Sm_N)} \times (Gd/Gd_N)]$. Normalizing values from Thompson (1982)

tFe_2O_3 total iron oxide as ferric iron, *LIO* loss on ignition, *A/CNK* molar $Al_2O_3/(CaO+Na_2O+K_2O)$

diffusion of major elements between the mafic and felsic magma, on the whole, tends towards a compositional equilibrium (Debon 1991). Therefore, in general, according to the fundamental principles of K, S and Na migrate from the felsic component towards the mafic one, while Ca, Fe, Mg, Ti, and Al migrate in the opposite direction (Best 1982; Debon 1991). The elements Na, K, Rb, Cs, Mg, Fe, Ca, Sr, and Ba have small ionic potential and are dissolved in the silicate melt as cations.

Discussion and petrogenetic approach

There are several theories about the formation of MMEs as mentioned in the first part. A widely accepted view for the genesis and evolution of MEEs is that they are resulted from mixing or mingling of mafic and crustal felsic magmas (e.g., Vernon 1984; Frost and Mahood 1987; Dorais et al. 1990; Blundy and Sparks 1992; Perugini et al. 2003; Barbarin 2005; Feeley et al. 2008). As a first approximation, petrographically chemical zoning of plagioclase, feldspar phenocrysts, acicular apatite, blade-like biotite, and mafic clots in both enclaves and host indicates that mixing process between mafic and felsic magmas strongly has been active. In addition, enclave various shapes (Fig. 3a, b) and irregular and dentate contact surfaces (Fig. 3e) imply to active magma-mixing phenomenon. MMEs irregular and angled margins suggest proximity to location of the active magma-mixing process (Didier and Barbarin 1991; Perugini et al. 2004; Troll et al. 2004). In addition, dentate borders among enclaves and their host rocks indicate fluid–fluid relation between them (Barnes et al. 2003; Lindline et al. 2004; Barbarin 2005). Furthermore, gradual and sharp contact surfaces in enclaves (Fig. 3d, e) show that process of the heat exchange was done in two slow and rapid stages. In the mixing place, variable degrees of elongation in metric sizes without any solid state deformation indicate variations in the viscosity of the enclaves, the time available for enclave deformation, and differential strain during the host granitoid magma flow (Arvin et al. 2004) and suggest that mafic enclaves and host rocks represent two co-existing distinct magmas (Kumar et al. 2004). MMEs feldspar phenocrysts which belong to the host granitoid reveal that the crystals grew in stirred coeval magmas of contrasting compositions (Slaby et al. 2008). Some researchers (e.g., Vernon 2004; Barbarin 2005; Browne et al. 2006) have suggested that such phenocrysts formed due to the thermal and chemical imbalance in semi-solid nature of enclave or resulted from mechanical transfer of mineral grains during the magma-mixing phenomena (Kumar et al. 2004). In addition, K-feldspar phenocrysts in the MMEs are rounded and similar in shape and size to those in the host, indicating crystal transportation from the host felsic magma into the mafic magma (e.g., Barbarin and Didier 1992; Waight et al. 2000; Perugini et al. 2003). This implies that there was only a small rheological difference between two magmas. As mentioned, the contact of mafic enclaves with host rocks is enriched in mafic material which might have nucleated and grown near margins due to a rapid drop in temperature of the enclave magma and due to selective diffusion of potassium and water, needed for hydrous amphibole and mica group of minerals to grow and which were

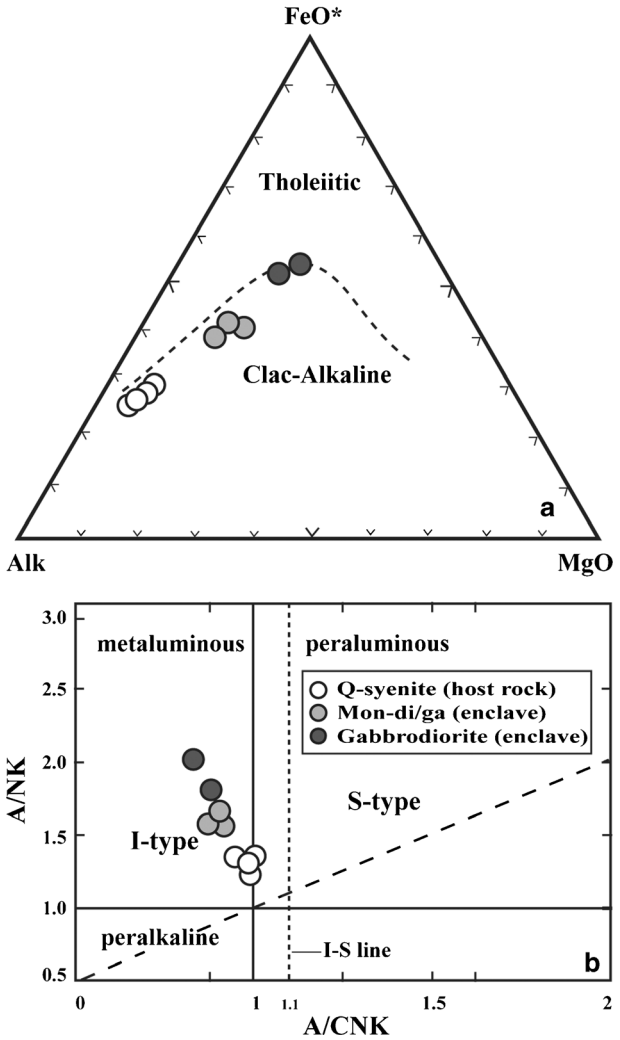

Fig. 7 **a** FeO*–Alk–MgO triangular diagram for dissociation of tholeiitic and calc-alkaline series (Irvine and Baragar 1971); **b** A/CNK vs. A/NK diagram for determination of the aluminum saturation index (Maniar and Piccoli 1989) and dissociation of I and S-type granites (Chappell and White 1974)

supplied from the adjacent granite melt saturated in these components (Johnston and Wyllie 1988; Wiebe 1994; Kumar et al. 2004).

Three hybridization stages can be defined according to their geochemical features by comparing the enclaves with reference diorite and quartz-diorite compositions, as given by Tindle (1991). The least hybridized enclaves are those with SiO_2 lower than 55 wt.% (Cj-42=47.27, Cj-44=42.68); the slightly hybridized are those with SiO_2 close to 56 wt.% (Cj-40=54.68, Cj-41=56.34, Cj-43=55.51), while the moderately hybridized are those with SiO_2 close to 58 wt.% (not present) (Table 1). The MMEs of gabbrodiorites and monzo-gabbro/diorites generally represent the least and slight hybridization stages with their felsic host rocks, respectively. The least hybridized stage may represent the most rapidly cooled magma, generally those with smaller dimensions that were affected mostly by addition of highly mobile elements (Van der laan and Wyllie 1993) such as K, Rb, and volatile components. Moreover, in this stage, large rheological and thermal differences between coeval felsic and mafic magmas inhibit much interaction and help in preserving features of the early two different magmas. The slightly hybridized stage may represent more slowly cooled MMEs.

As previously determined geochemically, all studied samples are calc-alkaline and have characteristics of I-type granitoids. Normally for continental arc magmas, a fundamental role is assigned to mantle-derived mafic magmas. They may be parental magmas, end members in mixing or assimilation processes, material for lower crustal source regions and heat sources that derived crustal melting (Tepper et al. 1993 and references therein). Furthermore, there is an emphasis on the fractional crystallization, crustal anatexis, and role of open system processes such as magma mixing and assimilation on the origin of granitic magmas (Tepper et al. 1993). The least hybridized MMEs in this study that may preserve the nature of parent magma, have low SiO_2 content (42 to 47 wt.%) and relatively high Mg no. (33 to 36) (Table 1), which suggests that the precursor of enclaves could be a basaltic magma. However, they have lower Ni (11–19 ppm) and Cr (95–102 ppm) relative to unfractionated basalt (200–450, and $N>1000$, respectively, Karsli et al. 2007). This suggests an ultramafic mantle source that underwent fractionation of olivine, pyroxene, and spinel prior to interaction with felsic magma. We believe that enclave-forming magmas were unlikely to originate from melting of a depleted mantle, followed by significant crustal contamination, because it would require incorporation of 35–52 % crustal components. Such a voluminous mixing/assimilation would significantly modify the major composition of these rocks. Therefore, the enclave-forming magmas were likely derived from an enriched mantle source, followed by variable degrees of hybridization with felsic components. This is in agreement with the marked high LILE and LREE of these samples (Fig. 10).

The host felsic rocks in the study area are dominated by quartz syenites. The origin of the felsic rocks has been a subject of many studies, and two main models have been proposed to interpret their petrogenesis: (1) pure crustal melts (e.g., Liu et al. 2002) or (2) mixture of crustal- and mantle-derived magmas (Chen and Zhai 2003; Yang et al. 2007). Both models are supported by our data. The host felsic rocks are characterized by high-K calc-alkaline features, high Sr and Ba amounts, and fractionated REE patterns with depleted HREE and negligible Eu anomalies (Fig. 10). These geochemical features are interpreted by the first model to form through partial melting of mafic lower crust at relatively high pressures. In addition, the principal arguments for the second model which were noted in the first paragraph strongly suggest the interaction of a mafic magma with a felsic magma. To further illustrate the magma-mixing process, a variation

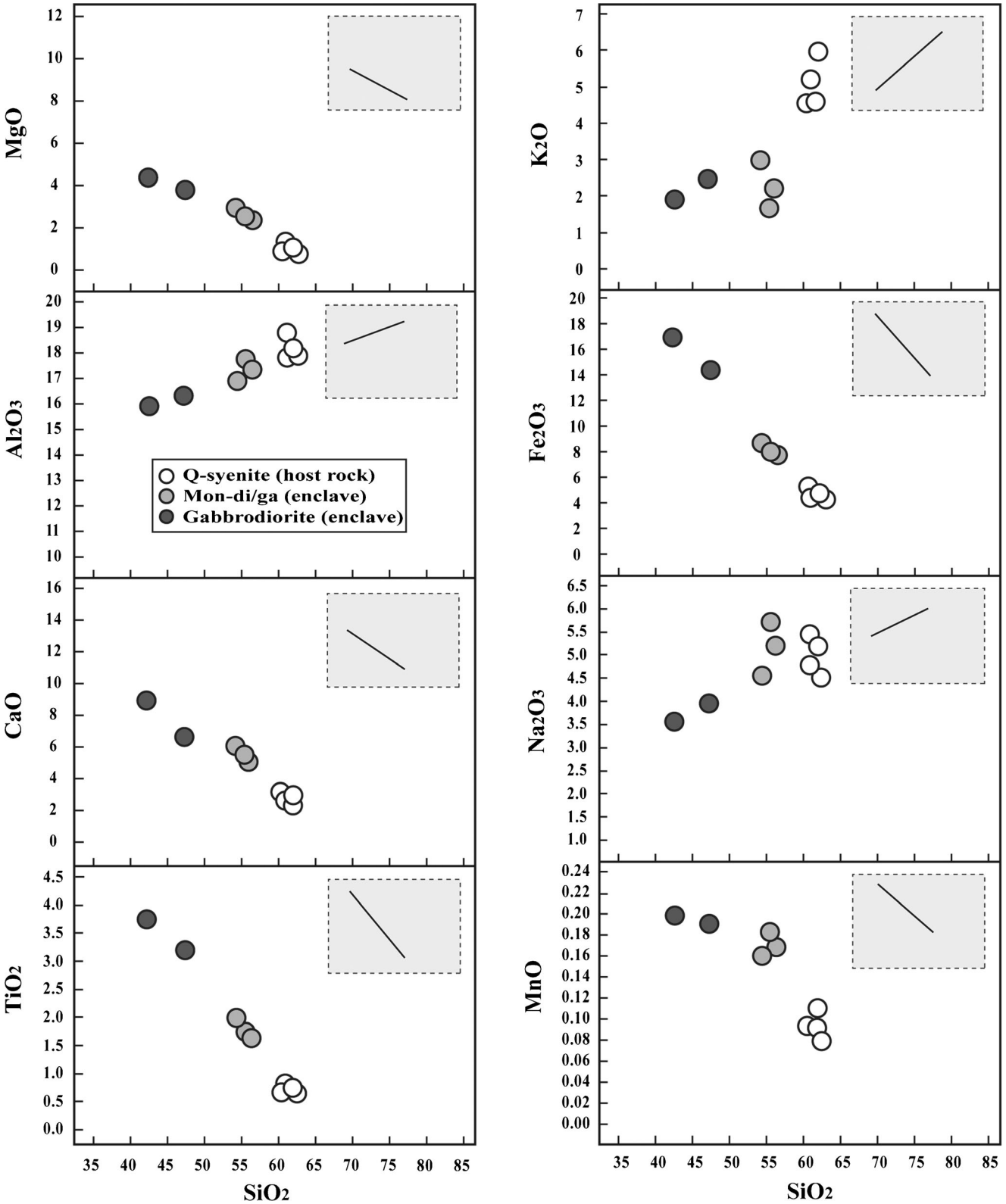

Fig. 8 Variation diagrams for selected major elements vs. silica for enclaves and host rocks

diagram of SiO_2 vs. Mg no. was constructed (Fig. 11) in which experimental melt field from melting of basalts (Rapp and Watson 1995) were plotted for comparison. It is noted that the host felsic rocks show significantly higher Mg no. than the experimental melts. This indicates that the felsic rocks are unlikely to be pure crustal melts, thus the first model could

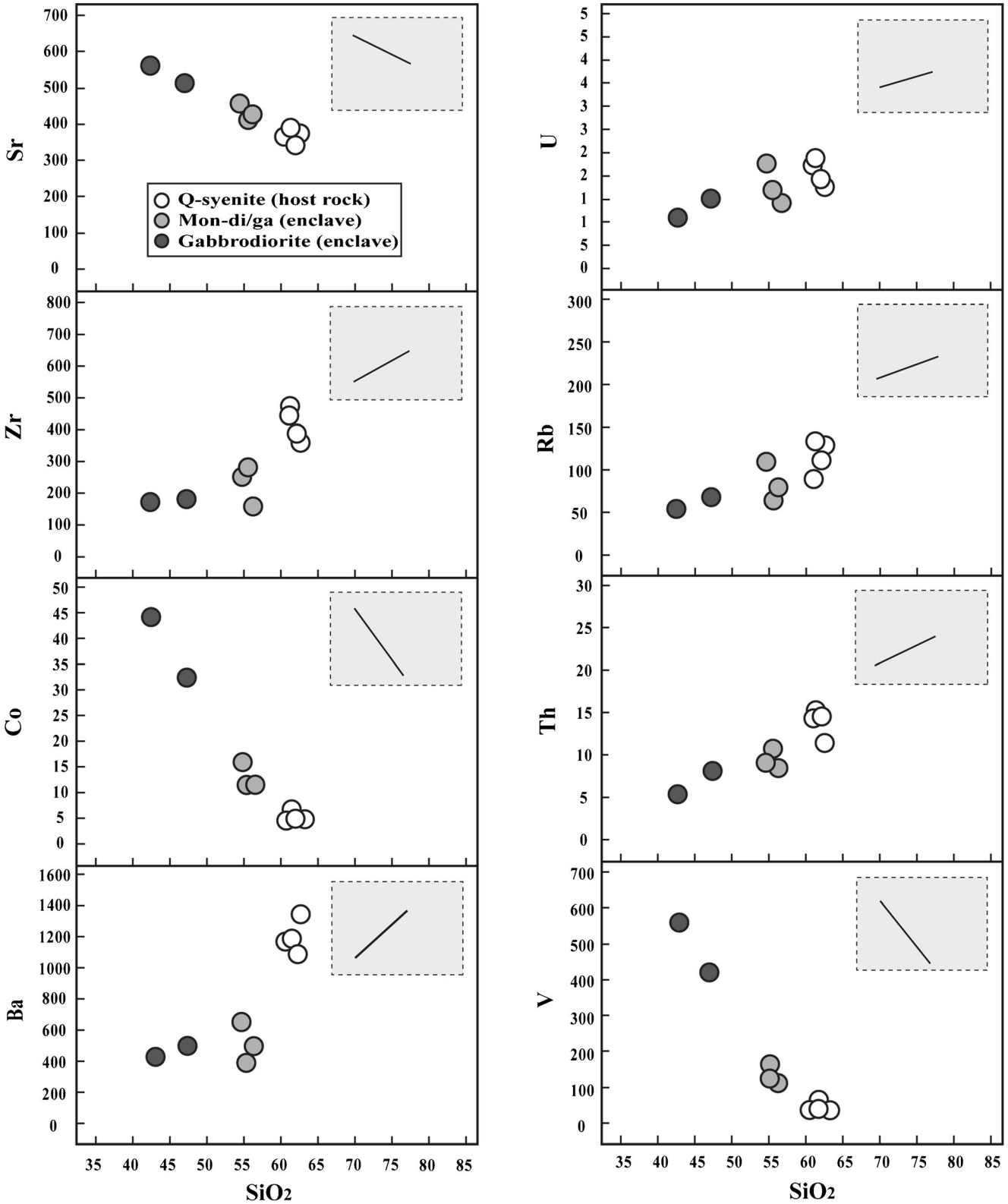

Fig. 9 Variation diagrams for selected trace elements vs. silica for enclaves and host rocks

be rejected. Particularly, relatively high Mg no. of the host felsic rocks can be generated during the incorporation of mantle-derived magma through hybridization (Chen et al. 2009). The coeval mafic magmas not only are intimately involved in the generation of the felsic magmas,but also provide thermal energy for crustal melting via fractional

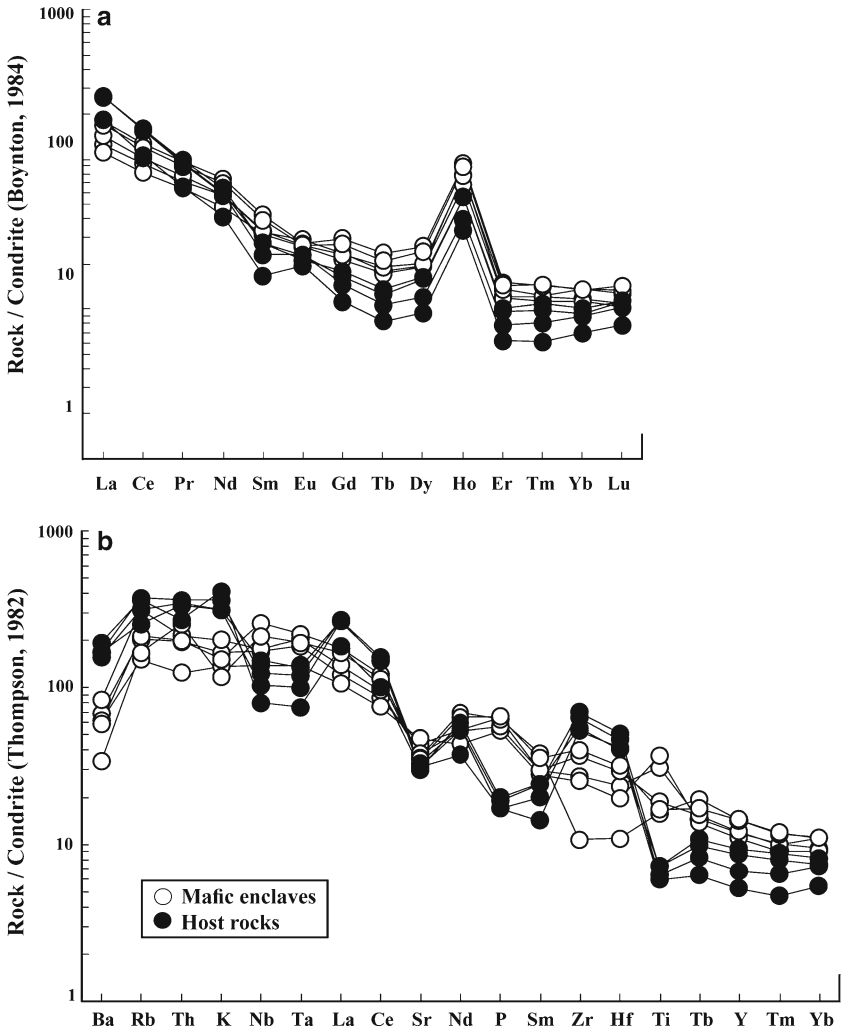

Fig. 10 **a** Chondrite-normalized REE; and **b** Multi-elements patterns for mafic enclaves and their host rocks (normalizing values are from Thompson 1982)

crystallization process. Considering the diagram of Nb/La vs. La/Yb (Abdel-Rahman and Nassar 2004) (Fig. 12), mafic and felsic samples have asthenospheric and lithospheric mantle origins, respectively. Therefore, we can conclude that petrogenesis of the mafic enclaves in the felsic plutons of the study area involves melting of the uppermost metasomatized

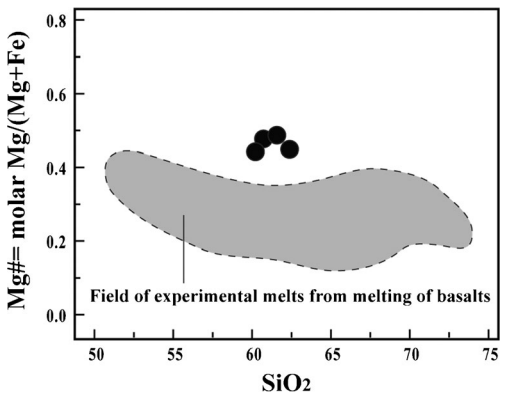

Fig. 11 Plot of SiO_2 vs. Mg no.. Host rocks are shown as *solid circles*, and the experimental melts from melting of basalts (Rapp and Watson 1995) as gray field. Note that host rocks have Mg no. higher than the experimental melts

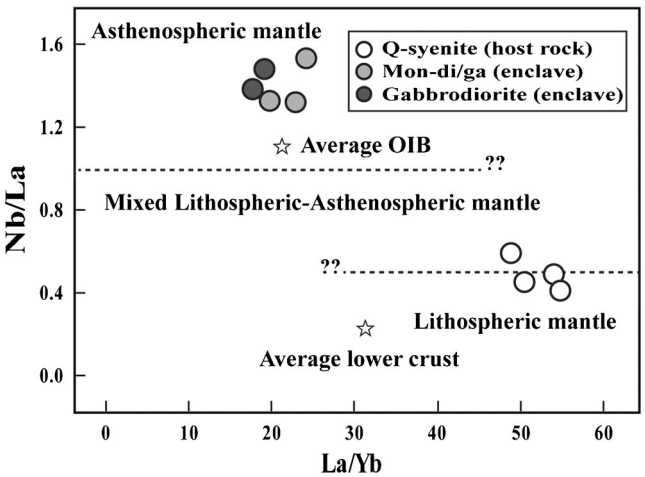

Fig. 12 Nb/La vs La/Yb diagram to distinguish of the lithospheric and asthenospheric mantle (Abdel-Rahman and Nassar 2004)

asthenosphere triggered by fluid fluxing from ancient subducted sediment. This melting resulted from formation of voluminous basaltic magma during magma ascent to the upper levels, forming enclave-forming magma and experienced significant fractionation of ferromagnesian phases like olivine and pyroxene. High-T mafic magma throughout its evolution produced the felsic q-syenite magma by fractional crystallization in lithospheric mantle. Large volume of mafic rocks relative to the felsic rocks in the study area (Fig. 2) are consistent with this interpretation and also homogenization process, where large proportions of mafic magma interact with a relatively small proportion of felsic melt (Frost and Mahood 1987). Consequently, neither significant crustal contamination nor mixing between mantle- and crustal-derived melts has been important (model 2 cited above), and those type of rocks are likely to have formed by fractional crystallization from a common mantle-derived parent. This is supported by elements linear trends and similar patterns in harker and spider diagrams respectively and approximately identical mineralogical composition of enclaves and host. Therefore, magma chemistry was effectively controlled by fractional crystallization only, despite the fact that the rocks slightly may have been affected by local crustal contamination given the low Sr, P, Ti, and high Rb, Th, K, and Cs (Fig. 10; Table 1). So, It can be concluded that mixing processes, involving the study granitoids, could have operated at two distinct, but continuous periods at different levels in the lithosphere: (1) thorough mixing at depth-formed homogeneous magmas that formed monzo-gabbro/diorites as intermediate enclaves as evidenced by concentration of transitional elements such as Ni, Cr, Cu, Zn, and V (Table 1) and (2) mingling and local mixing during ascent and emplacement.

Conclusions

The combination of field, textural, and whole-rock chemical evidence leads to the conclusion that magma mixing and mingling of mafic and felsic magmas played an important role in the petrogenesis of the studied intrusion. Enclaves enclosed in q-syenite, although strongly more mafic, are chemically very similar to their host. MMEs have structures and textures that show significant magma-mixing and mingling processes. Enclaves at various shapes and sizes, irregular, gradual, and sharp contact surfaces, finer-grained enclaves, and areas enriched in mafic material, feldspar phenocrysts belonging to host in enclaves, chemical zoning of plagioclase, resorbed plagioclase rims, acicular apatite, blade-like biotite, and mafic clots strongly indicate mixing and mingling of co-existing mafic and felsic magmas with liquid–liquid relation. The study of the enclaves demonstrates that MMEs are hardly informative about the original mafic magma composition. The MMEs under study are composed predominantly of gabbrodiorite and monzo-gabbro/diorite along with host displaying mineralogical and geochemical characteristics of I-type granitoids. Our investigation shows that the enclave-forming magma may have originated from uppermost metasomatized asthenosphere and formed from a basaltic magma after fractionation of some phases such as olivine, pyroxene, and spinel prior to interaction with felsic magma. In addition, MMEs and hosts with similar chemical and mineralogical compositions, large mafic mass volume relative to the felsic unit along with occurrence of homogenization process indicate that felsic part might have been produced by fractional crystallization from enclave-forming mafic magma without significant crustal contamination. Indeed, enclaves and host rocks more likely originated from a single basaltic parent magma. This is in agreement with the marked high Mg no., LILE and LREE enclave, and host samples. Finally, coeval mafic and felsic magmas may have evolved at two distinct but continuous periods at different levels (before and during ascent and emplacement) as a result of the combined multistage interactions (least and slight hybridization stages), which are commonly represented by basic to hybrid MMEs.

Acknowledgments Financial support from the Iranian Ministry of Science, Research and Technologyis and from the University of Urmia (Iran) is gratefully acknowledged. The authors like to thank Editors of Arabian Journal of Geosciences and reviewers of the paper for their efforts.

References

Abdel-Rahman AFM, Nassar PE (2004) Cenozoic volcanism in the Middle East: petrogenesis of alkali basalts from northern Lebanon. Geol Mag 141:545–563

Agard P, Omrani J, Jolivet L, Whitechurch H, Vrielynck B, Spakman W, Monie P, Meyer B, Wortel R (2011) Zagros orogeny: a subduction-dominated process. Geol Mag 148:692–725

Alavi M (1994) Tectonic of the Zagros orogenic belt of Iran: new data and interpretations. Tectonophysics 229:211–238

Alavi M, Mahdavi MA (1994) Stratigraphy and structures of the Nahavand region in western Iran and their implications for the Zagros tectonics. Geol Mag 131:43–47

Alavi M, Vaziri H, Seyed-Emami K, Lasemi Y (1997) The Triassic and associated rocks of the Nakhlak and Aghdarband areas in central and northeastern Iran as remnants of the southern Turonian active continental margin. Geol Soc Am Bull 109:1563–1575

Alirezaei S, Hassanzadeh J (2012) Geochemistry and zircon geochronology of the Permian A-type hasanrobat granite, Sanandaj-Sirjan belt: a new record of the Gondwana break-up in Iran. Lithos 151:122–134

Allen CM (1991) Local equilibrium of mafic enclaves and granitoids of the Turtle pluton, southeast California: mineral, chemical and isotopic evidence. Am Mineral 76:574–588

Arvin M, Dargahi S, Babaei AA (2004) Mafic microgranular enclave swarms in the Chenar granitoid stock, NW of Kerman, Iran: evidence for magma mingling. J Asian Earth Sci 24:105–113

Azizi H, Jahangiri A (2008) Cretaceous subduction-related volcanism in the northern Sanandaj-Sirjan zone, Iran. J Geodyn 45:178–190

Bacon CR (1986) Magmatic inclusions in silicic and intermediate volcanic rocks. J Geophys Res 91:6091–6112

Barbarin B (2005) Mafic magmatic enclaves and mafic rocks associated with some granitoids of the central Sierra Nevada batholith, California: nature, origin, and relations with the hosts. Lithos 80: 155–177

Barbarin B, Didier J (1992) Genesis and evolution of mafic microgranular enclaves through various types of interaction between coexisting felsic and mafic magmas. Trans R Soc Edinb Earth Sci 83:145–153

Barnes CG, Prestvik T, Barnes MA, Anthony EY, Allen CM (2003) Geology of a magma transfer zone: the hortavaer igneous complex, north-central Norway. Nor J Geol 83:187–208

Bebien J (1991) Enclaves in plagiogranites of the Guevgueli ophiolitic complex, Macedonia, Greece. In: Didier J, Barbarin B (eds) Enclaves and granite petrology. Elsevier Science Publisher B.V, Amsterdam, pp 205–219

Berberian M (1977) Three phases of metamorphism in Haji-Abad quadrangle (southern extremity of the Sanandaj–Sirjan structural Zone): a palaeotectonic discussion. In: Berberian M (ed) Contribution to the Seismotectonics of Iran (part III). Geological Survey of Iran, Report 40, Tehran, pp 239–263

Berberian M, King GCP (1981) Towards a paleogeography and tectonic evolution of Iran. Can J Earth Sci 18:210–265

Best M (1982) Igneous and metamorphic petrology. Freeman, San Francisco, p 630

Blundy JD, Sparks RSJ (1992) Petrogenesis of mafic inclusions in granitic rocks of the Adamello massif, Italy. J Petrol 33:1039–1104

Browne BL, Eichelberger JC, Patino LC, Vogel TA, Uto K, Hoshizumi H, Dehn J (2006) The generation of porphyritic and equigranular enclaves during magma recharge events at Unzen volcano, Japan. J Petrol 47:301–328

Chappel BW, White AJR (1992) I- and S-types granites in the Lachland fold belt. Trans R Soc Edinb Earth Sci 83:1–26

Chappell BW, White AJR (1974) Two contrasting granite types. Pac Geol 8:173–174

Chappell BW, White AJR, Wyborn D (1987) The importance of residual source material (restite) in granite petrogenesis. J Petrol 28:1111–1138

Chen B, Zhai MG (2003) Geochemistry of late Mesozoic lamprophyre dykes from the Taihang Mountains, north China, and implications for the sub-continental lithospheric mantle. Geol Mag 140:87–93

Chen B, Chen ZC, Bor-Ming J (2009) Origin of mafic enclaves from the Taihang Mesozoic Orogen, North China Craton. Lithos 110:1–4

Dahlquist JA (2002) Mafic microgranular enclaves: early segregation from metaluminous magma (Sierra de Chepes), Pampean Ranges, NW Argentina. J S Am Earth Sci 15(6):643–655

Debon F (1991) Comparative major element chemistry in various "microgranular enclave-plutonic host" pairs. In: Didier J, Barbarin B (eds) Enclaves and granite petrology. Developments in Petrology, Elsevier, Amsterdam, pp 293–312

Didier J (1973) Granites and their enclaves. Elsevier, London, p 393

Didier J, Barbarin B (1991) The different types of enclaves in granites—nomenclature. In: Didier J, Barbarin B (eds) Enclaves and granite petrology. Developments in Petrology, Elsevier, Amsterdam, pp 19–24

Dodge FCW, Kistler RW (1990) Some additional observations on inclusions in the granitic rocks of the Sierra Nevada. J Geophys Res 95: 17841–17848

Donaire T, Pascual E, Pin C, Duthou JL (2005) Microgranular enclave as evidence of rapid cooling in granitoid rocks: the case of the Los Pedroches granodiorite, Iberian Massif, Spain. Contrib Mineral Petrol 149(3):247–265

Dorais MJ, Whitney JA, Roden MF (1990) Origin ofmafic enclaves inthe Dinkey Creek Pluton, Central Sierra Nevada batholith, California. J Petrol 31:853–881

Feeley TC, Wilson LF, Underwood SJ (2008) Distribution and compositions magmatic inclusions in the Mount Helen dome, Lassen volcanic center, California: insights into magma chamber processes. Lithos 106:173–189

Fernandez AN, Barbarin B (1991) Relative rheology of coeval mafic and felsic magmas: nature of resulting iteraction processes and shape and mineral fabrics of mafic microgranular enclaves. In: Didier J, Barbarin B (eds) Enclaves and granite petrology, vol 13. Developments in petrology, Elsevier, Amsterdam, pp 263–275

Frost TP, Mahood GA (1987) Field, chemical, and physical constraints on mafic-felsic magma interaction in the Lamark Granodiorite, Sierra Nevada, California. Geol Soc Am Bull 99:272–291

Golonka J (2004) Plate tectonic evolution of the southern margin of Eurasia in the Mesozoic and Cenozoic. Tectonophysics 381:235–273

Hibbard MJ (1981) The magma mixing origin of mantled feldspars. Contrib Mineral Petrol 76:158–170

Holden P, Halliday AN, Stephens WE, Henney PJ (1991) Chemical and isotopic evidence for major mass transfer between mafic enclaves and felsic magma. Chem Geol 92:135–152

Ilbeyli N, Pearce JA (2005) Petrogenesis of igneous enclaves in plutonic rocks of the central Anatolian Massif, Turkey. Int Geol Rev 47: 1011–1034

Irvine TN, Baragar WRA (1971) A guid to chemical classification of the common volcanic rocks. Can J Earth Sci 8:523–548

Johnston AD, Wyllie PJ (1988) Interaction of granitic and basic magmas: experimental observations on contamination processes at 10 kbar with H, O. Contrib Mineral Petrol 98:352–362

Karsli O, Chen B, Aydin F, Sen C (2007) Geochemical and Sr–Nd–Pb isotopic compositions of the Eocene Dölek and Sariçiçek Plutons, Eastern Turkey: implications for magma interaction in the genesis of high-K calc-alkaline granitoids in a post-collision extensional setting. Lithos 98:67–96

Kaygusuz A, Aydıncakır E (2009) Mineralogy, whole-rock and Sr–Nd isotope geochemistry ofmafic microgranular enclaves in Cretaceous Dagbasi granitoids, Eastern Pontides, NE Turkey: evidence of magmamixing, mingling and chemical equilibration. Chem Erde 69:247–277

Kumar S, Rino V, PAL AB (2004) Field evidence of magma mixing from microgranular enclaves hosted in Palaeoproterozoic Malanjkhand granitoids, central India. Gondwana Res 7:539–548

Lindline J, Crawford WA, Crawford ML (2004) Bimodal volcanic-plutonic system: the Zarembo Island extrusive suite and the Burnett Inlet intrusive complex. Can J Earth Sci 41:355–375

Liu HT, Sun SH, Liu JM, Zhai MG (2002) The Mesozoic high-Sr granitoids in the northern marginal region of North China craton: geochemistry and source region. Acta Petrol Sin 18:257–274

Maniar PD, Piccoli PM (1989) Tectonic discrimination of granitoids. Geol Soc Am Bull 101:635–643

Masoudi F, Yardley BWD, Cliff RA (2002) Rb–Sr geochronology of pegmatites, plutonic rocks and hornfels in the region southwest of Arak. Islam Repub Iran J Sci 13:249–254

Mohajjel M, Fergusson CL (2000) Dextral transpression in Late-Cretaceous continental collision, Sanandaj–Sirjan zone, Western Iran. J Struct Geol 22:1125–1139

Mohajjel M, Fergusson CL, Sahandi MR (2003) Cretaceous-Tertiary convergence and continental collision, Sanandaj-Sirjan Zone, western Iran. J Asian Earth Sci 21:397–412

Molinaro M, Zeyen H, Laurencin X (2005) Lithospheric structure underneath the SE Zagros mountains, Iran: recent slab breakoff ? Terra Nova 25:1–6

Mouthereau F, Lacombe O, Verges J (2012) Building the Zagros collisional orogen: timing, strain distribution and the dynamics of Arabia/Eurasia plate convergence. Tectonophysics 532–535: 27–60

Naghizadeh R, Ghalamghash J (2005) Geological map of Oshnavieh 1: 100,000, Geological Survey of Iran

Nezafati N, Herzig PM, Pernicka E, Momenzadeh M (2005) Intrusion-related gold occurrences in the Astaneh-Sarband area, west central Iran. In: J. Mao and F. P. Bierlein (eds.) Mineral deposit research:

meeting the global challenge. Springer, pp 445–448, DOI: 10.1007/3-540-27946-6_116

Pabst A (1928) Observations on inclusions in the granitic rocks of the Sierra Nevada. Univ Calif Publ: Dep Geol Sci 17:325–386

Parada MA, Nystrom JO, Levi B (1999) Multiple sources for the Coastal Batholith of central Chile (31–34S): geochemical and Sr–Nd isotopic evidence and tectonic implications. Lithos 46:505–521

Perugini D, Poli G, Christofides G, Eleftheriadis G (2003) Magma mixing in the Sithonia plutonic complex, Greece: evidence from mafic microgranular enclaves. Mineral Petrol 78:173–200

Perugini D, Ventura G, Petrelli M, Poli G (2004) Kinematic significance of morphological structures generated by mixing of magmas: a case study from Salina Island (Southern Italy). Earth Planet Sci Lett 222: 1051–1066

Pin C, Binon M, Belin J, Barbarin B, Clemens JD (1990) Origin of microgranular enclaves in granitoids: equivocal Sr–Nd evidence from Hercynian rocks in the Massif Central (France). J Geophys Res 95:17821–17828

Platevoet B, Bonin B (1991) Enclaves and mafic-felsic associations in the Permian alkaline province of Corsica, France: physical and chemical interactions between coeval magmas. In: Didier J, Barbarin B (eds) Enclaves and granite petrology, developments in petrology. Elsevier, Amesterdam, pp 191–204

Rachidnejad-Omran N, Emami MH, Sabzehei M, Rastad E, Bellon H, Pique A (2002) Lithostratigraphie et histoire paléozoïque à paléocène des complexes métamorphiques de la région de Muteh, zone de Sanandaj–Sirjan (Iran méridional). C R Acad Sci 334:1185–91

Rapp RP, Watson EB (1995) Dehydration melting of metabasalt at 8–32 kbar: implications for continental growth and crust–mantle recycling. J Petrol 36:891–931

Ricou LE (1994) Tethys reconstructed: plates continental fragments and their boundaries since 260 Ma from central America to Southeastern Asia. Geodin Acta 7:169–218

Sengor AMC (1990) A new model for the late Paleozoic–Mesooic tectonic evolution of Iran and implications for Oman. In: Robertson AHF, Searle MP, Ries AC (eds) The geology and tectonics of the Oman Region, vol 22. Geological Society of London, Special Publication, London, pp 278–281

Shahbazi H, Siebel W, Pourmoafee M, Ghorbani M, Sepahi AA, Shang CK, Vousoughi A (2010) Geochemistry and U-Pb geochronology of the Alvand plutonic complex in Sanandaj-Sirjan Zone (Iran): new evidence for Jurassic magmatism. J Asian Earth Sci 39: 668–683

Shahrabi M, Saidi A (1985) Geological Map of Urumieh 1:250,000 Quadrangle Map Iran N^{o}, vol. B3. Geological Survey of Iran

Shaw A, Downes H, Thirwall MF (1993) The quartz-diorites of Limousin: elemental and isotopic evidence for Devono-Carboniferous subduction in the Hercynian belt of the French Massif Central. Chem Geol 107:1–18

Silva MMVG, Neiva AMR, Whitehouse MJ (2000) Geochemistry of enclaves and host granites from the Nelas area, central Portugal. Lithos 50:153–170

Slaby E, Goetze J, Worner G, Simon K, Wrzalik R, Michal S (2008) K-feldspar phenocrysts in microgranular magmatic enclaves; a cathodoluminescence and geochemical study of crystal growth as a marker of magma mingling dynamics. Lithos 105:1–2

Stocklin J (1968) Structural history and tectonics of Iran: a review. Am Assoc Pet Geol Bull 52:1229–1258

Streckeisen AL (1973) Plutonic rocks, classification and nomenclature recommended by the IUGS subcommission on the systematics of igneous rocks. Geotimes 18:26–30

Takin M (1972) Iranian geology and continental drift in the Middle East. Nature 235:147–150

Tepper JH, Nelson BK, Bergantz GW, Irving AJ (1993) Petrology of the Chilliwack batholith, North Cascades, Washington: generation of calc-alkaline granitoids by melting of mafic lower crust with variable water fugacity. Contrib Mineral Petrol 113:333–351

Thompson AB (1982) Magmatism of the British tertiary volcanic province. Scott J Geol 18:49–107

Tindle AG (1991) Trace element behaviour in microgranular enclaves from granitic rocks. In: Didier J, Barbarin B (eds) Enclaves and granite petrology. Developments in Petrology, Elsevier, Amsterdam, pp 313–331

Topley CG, Brown M, Power GM (1982) Interpretations of field relationships of diorites and associated rocks with particular reference to northwest Guernsey, Channel Islands. Geol J 17:323–343

Troll VR, Donaldson CH, Emeleus CH (2004) Pre-eruptive magma mixing in intra-caldera ash-flow deposits of the Rum Igneous Centre, Scotland. Contrib Mineral Petrol 147:722–739

Van der laan SR, Wyllie PJ (1993) Experimental interaction of granitic and basaltic magmas and implications for mafic enclaves. J Petrol 34:491–517

Vernon RH (1983) Restite, xenoliths and microgranitoid enclaves in granites. J Proc Royal Soc New South Wales (Australia) 116:77–103

Vernon RH (1984) microgranitoid enclaves in granite-globules of hybrid magma quenched in a plutonic environment. Nature 309:438–439

Vernon RH (1991) Interpretation of microstructures of microgranitoid enclaves. In: Didier J, Barbarin B (eds) Enclaves and granite petrology. Developments in Petrology, Elsevier, Amsterdam, pp 277–291

Vernon RH (2004) A practical guide to rock microstructure. Cambridge University Press, Cambridge, p 594

Waight TE, Maas R, Nicholls IA (2000) Fingerprinting feldspar phenocrysts using crystal isotopic composition stratigraphy: implications for crystal and magma mingling in S-type granites. Contrib Mineral Petrol 139:227–239

White RV, Tarney J, Kerr AC, Saunders AD, Kempton PD, Pringle MS, Klaver GT (1999) Modification of an oceanic plateau, Aruba, Dutch Caribbean: implications for the generation of continental crust. Lithos 46:43–68

Wiebe RA (1994) Silicic magma chambers as traps for basaltic magmas: the Cadillac mountain intrusive complex, Mount Desert island, Maine. J Geol 102:423–427

Yang JH, Fu-Yuan Wu FY, Wilde SA, Xie LW, Yang YH, Liu XM (2007) Tracing magma mixing in granite genesis: in situ U–Pb dating and Hf-isotope analysis of zircons. Contrib Mineral Petrol 153:177–190